Steric Effects and Solvent Effects on S(N)2 Reactions

ARTICLE *in* THE JOURNAL OF PHYSICAL CHEMISTRY A · SEPTEMBER 2009

Impact Factor: 2.69 · DOI: 10.1021/jp905429p · Source: PubMed

3 AUTHORS, INCLUDING:

Christopher J Cramer
University of Minnesota Twin Cities
532 PUBLICATIONS **23,506** CITATIONS
SEE PROFILE

Donald Truhlar
University of Minnesota Twin Cities
1,342 PUBLICATIONS **81,884** CITATIONS
SEE PROFILE

Steric Effects and Solvent Effects on S_N2 Reactions

Yongho Kim,[†,‡] Christopher J. Cramer,[‡] and Donald G. Truhlar*[,‡]

Department of Chemistry, Kyung Hee University, 1 Seochun-dong, Kiheung-Gu, Yongin, Gyeonggi-Do, 449-701, Korea, and Department of Chemistry and Supercomputing Institute, University of Minnesota, 207 Pleasant Street Southeast, Minneapolis, Minnesota 55455-0431

Received: June 10, 2009

We present quantum mechanical calculations designed to disentangle the influences of solvent effects and substituent effects on ionic nucleophilic substitution reactions. In particular, we compare the S_N2 reactions of Cl^- with $CH_3CH(X)Cl$ and $(CH_3)_3CCH(X)Cl$ for X = H and CN in the gas phase and aqueous solution. We find that, for all of these reactions, transition state distortion and dielectric descreening effects are quantitatively larger in magnitude than hydrophobic effects or exchange repulsion, but they also roughly cancel one another so that differential solvation contributes little to differences in the free energies of activation associated with a CH_3 versus a $(CH_3)_3C$ group as a substituent at the reacting position. Differential solvation of the transition-state structures relative to the reactants is less unfavorable for X = H than for X = CN because of the greater charge separations in the X = H case, and this separation places more positive charge on the reacting carbon center. The smaller deceleration associated with aqueous solvation for X = H roughly balances the gas-phase acceleration predicted for X = CN so that the aqueous activation free energies for the substrates are predicted to be similar for these two substituents.

1. Introduction

It has long been known[1] that liquid-phase bimolecular nucleophilic substitution (S_N2) reactions of substituted alkyl halides RCH_2Y (where Y is a halogen) proceed more slowly when R is a larger alkyl group than when it is a smaller one (or a hydrogen). The largest difference between successive homologues RCH_2Y is for R = H and R = CH_3, and smaller differences are observed between the increasingly larger alkyl groups. This trend associated with β-substitution was originally interpreted in terms of a steric effect: large groups R effectively block the backside approach of the incoming nucleophile to the reactive methylene carbon.[2] The influence of a polar effect, that is, an effect associated with differences in electron-donating tendencies for different alkyl groups, was discounted owing to the β relationship between these groups and the reactive center. This analysis for RCH_2Y systems thus contrasted β-substitution effects with α-substitution effects (i.e., effects associated with the variation of alkyl groups R in reactants R_3CY), since polar effects were considered to be quite important for the latter.[2] An additional consideration is that it has long been recognized that solvation retards the rate of any particular S_N2 reaction of the form $X^- + RCH_2Y \rightarrow RCH_2X + Y^-$ because charge is distributed more widely in the "critical complex" (now called the transition state or TS) than in the reactants.[1]

Quantitatively, the Arrhenius activation energies relative to R = H for the S_N2 reactions of EtO^- with RCH_2Br in ethanol were found to be 1.0, 1.4, 2.8, and 6.2 kcal/mol for R = CH_3, CH_3CH_2, $(CH_3)_2CH$, and $(CH_3)_3C$, respectively. These differences served to stimulate theoretical models focusing on steric hindrance.[2] In the present article, we use "steric" in the traditional sense of a direct interaction between two groups due to exchange repulsion.

Although early work did not attribute any portion of substitution effects (e.g., Me vs Et) to differential solvation effects, we now recognize that increasingly bulky nonpolar substituents affect solvation free energies by a noninductive, nonsteric effect called solute descreening. Thus, a solvent screens the Coulomb interactions between separated (partial) charges in solutes, with the magnitude of the screening being proportional to the solvent's dielectric constant, so that a more polar solvent more effectively screens charge−charge interactions such as those between polar functional groups. However, a large alkyl group near a polar functional group prevents the close approach of solvent to the latter and thereby acts to descreen the polar group.[3] Depending on the process in question, differential descreening effects may have magnitudes equal to or larger than classic polar or steric effects.

A considerable amount of modern work on S_N2 reactions has been motivated by the search for an understanding of intrinsic reactivity, defined as "chemical behavior in a solvent-free environment."[4] As a further step toward focusing on intrinsic characteristics, one can especially consider symmetric reactions, for which the free energy of activation relative to the encounter complex corresponds to the intrinsic free energy of activation of Marcus theory.[5] Regan et al.[6] measured rates of the nearly symmetric $^{37}Cl^- + CH_3CH(CN)^{35}Cl$ (**R1**) and $^{37}Cl^- + (CH_3)_3CCH(CN)^{35}Cl$ (**R2**) S_N2 reactions in the gas phase and inferred by a statistical treatment of the rate constants that the relevant barrier heights are −1.6 and 0.0 kcal/mol, respectively (note that a small negative *energy* barrier in such reactions is still associated with a rate-controlling dynamical bottleneck because the *free energy* of activation is positive). This difference, 1.6 kcal/mol, is smaller than the 5.2 kcal/mol energetic difference mentioned above for the reactions of CH_3CH_2Br and $(CH_3)_3CCH_2Br$ with EtO^- in ethanol. To explain this, Regan et al.[6] calculated (using a Monte Carlo explicit-solvent simulation method[7]) the difference in the aqueous solvation contribution to the free energy of activation for these two reactions and found

* Corresponding author. E-mail: truhlar@umn.edu.
† Kyung Hee University.
‡ University of Minnesota.

10.1021/jp905429p CCC: $40.75
Published on Web 07/23/2009

that the solvation effect is 4.0 kcal/mol more positive (retarding) for the R = $(CH_3)_3C$ case than the R = CH_3 case. The conclusion was that there is an intrinsic steric effect, but the aqueous reaction is slowed down primarily by solvation and only secondarily by nonbonded interactions that could be labeled steric effects.

The question of steric retardation of S_N2 reactions in the gas phase and solution was subsequently re-examined by Vayner et al.[8] They first calculated gas-phase standard-state enthalpies of activation $\Delta^{\ddagger}H_0$ by the CBS-QB3//B3LYP/6-311G(2d,d,p) method[9] for the two S_N2 reactions studied by Regan et al. plus three other reactions. Their $\Delta^{\ddagger}H_0$ values were −0.6 and 5.7 kcal/mol for (**R1**) and (**R2**), respectively—with the former in reasonable agreement with experiment and the latter in poor agreement with experiment, casting doubt on the experiment or its interpretation and the conclusions drawn from it. Vayner et al.[8] also calculated the standard-state free energy of activation $\Delta^{\ddagger}G_{298}$ in both the gas phase and the aqueous solution, with solvation treated by the CPCM[10] implicit solvent model. They found $\Delta^{\ddagger}G_{298}$ for **R1** and **R2** equal to 6.3 and 12.6 kcal/mol, respectively, in the gas phase, and 40.5 and 46.9 kcal/mol, respectively, in solution. The gas-phase difference of 6.3 kcal/mol is about equal to the solution difference of 6.4 kcal/mol, in opposition to the conclusion of Regan et al. with respect to a presumed large solvation effect. They inferred that the conclusions of ref 6 are most likely not true.

We decided to re-examine these reactions with theoretical methods designed to ensure convergence of the gas-phase energetics with respect to electron correlation and a one-particle basis set and also to address the influence of solvent using models demonstrated to be highly accurate for the prediction of aqueous free energies of solvation. We report here the results of these re-investigations.

2. Theory

We consider only a temperature T of 298 K.

The standard-state free energies of species X in the gas phase (g) and aqueous solution (aq) are related by[10]

$$G\ (\mathrm{X,aq}) = G\ (\mathrm{X,g}) + \Delta G_S^{\circ}(\mathrm{X}) \qquad (1)$$

where ΔG_S is the standard-state free energy of solvation. Summing eq 1 over products and subtracting the sum over reactants give the standard-state free energy of reaction:

$$\Delta G\ (\mathrm{aq}) = \Delta G\ (\mathrm{g}) + \Delta\Delta G_S^{\circ} \qquad (2)$$

The analogue of eq 2 for the standard-state free energy of activation is

$$\Delta^{\ddagger}G\ (\mathrm{aq}) = \Delta^{\ddagger}G\ (\mathrm{g}) + \Delta^{\ddagger}\Delta G_S^{\circ} \qquad (3)$$

where $\Delta^{\ddagger}G$ is the free energy of the transition state (which is missing one degree of freedom) minus the sum of the free energies of reactants and $\Delta^{\ddagger}\Delta G_S$ is the difference between the free energy of solvation of the transition state and the sum of the free energies of solvation of the reactants. The transition state should be variationally optimized,[12] but for typical symmetric S_N2 reactions, which include those studied here, the variational transition state is the same as the conventional one. Therefore, we apply conventional transition state theory here, in which case the gas-phase transition state is located at a saddle point on the gas-phase potential energy surface,[13] and in the equilibrium solvation path approximation, the liquid-phase transition state is located at a saddle point on the solute potential of mean force.[14]

For clarity, in various contexts one might add a subscript T or a subscript value of the temperature to the free energies of eqs 1−3 when it is desirable to emphasize the temperature.

The standard-state free energy of solvation may be written as

$$\Delta G_S^{\circ}(\mathrm{X}) = \Delta G_S^{*}(\mathrm{X}) + \Delta G_{\mathrm{conc}} \qquad (4)$$

where $\Delta G_S^{*}(\mathrm{X})$ corresponds to the solvation free energy in a process in which the concentration of solute X is the same in the gas phase and a dilute liquid (for such a process the solvation free energy is directly related to the work of coupling a single X in dilute solution to the solvent[15]) and ΔG_{conc} is the free energy required to bring the concentrations to their standard-state values. Here we use standard states of a 1 atm ideal gas and a 1 M ideal solution, for which $\Delta G_{\mathrm{conc}} = +1.89$ kcal/mol.

We calculate G (X,g) in the Born−Oppenheimer approximation as the potential energy and vibrational zero point energy plus the thermal electronic−vibrational−rotational−translational free energy. All vibrational−rotational contributions are calculated in the harmonic oscillator rigid rotator approximation.

We calculate $\Delta G_S^{*}(\mathrm{X})$ by an implicit solvation model,[11] in particular by the SM8[16] solvation model. In this model, we have[11,16,17]

$$\Delta G_S^{*} = \Delta G_{\mathrm{ENP}} + G_{\mathrm{CDS}} \qquad (5)$$

where

$$\Delta G_{\mathrm{ENP}} = \Delta E_{\mathrm{EN}} + G_P \qquad (6)$$

In these equations, G_P is the free energy of polarizing the solute (equal to the favorable solute−solvent interaction energy in the equilibrium polarized state minus the cost of polarizing the solvent[18]), ΔE_{EN} is the potential energy cost of raising the internal energy of the solute by geometric and electronic distortion to reach the most favorable polarized state in the liquid-phase solute, and G_{CDS} is the cavity-dispersion-solvent structure term. G_P is calculated electrostatically using the bulk electrostatic dielectric constant of the solvent,[11,16,17] but since the solvation free energy is not rigorously separable into electrostatic and nonelectrostatic terms,[19] G_{CDS} is parametrized[16] to be consistent with the assumed bulk electrostatic model; thus, G_{CDS} also includes the nonbulk electrostatic component of the solvation free energy. We note that the deviation of hydrogen bonding from that predicted by bulk electrostatics is included in the solvent structure component of G_{CDS}, and dielectric descreening (which was mentioned already in the introduction) is contained in G_P by using a realistic solute cavity.[20] A key aspect of the calculation of G_P is that it includes a realistic description of the size and shape of the solute cavity for both the reactants and the transition state.[11]

3. Methods

The first set of calculations was carried out by hybrid Kohn−Sham density functional theory[21] with the M06-2X density functional[22] and the 6-31+G(d,p) basis set.[23] Solvation

TABLE 1: Gas-Phase Energetics (kcal/mol)

	$V^{\ddagger}$		$\Delta^{\ddagger}H_0$		$\Delta^{\ddagger}G_{298}$	
method	**R1**	**R2**	**R1**	**R2**	**R1**	**R2**
CBS-QB3[a]	n.a.[b]	n.a.	−0.6	5.7	6.3	12.6
M06-2X	−0.5	6.0	−0.9	5.6	6.4	14.0
BMC//M06-2X	−0.4	5.6	−0.8	5.2	6.5	13.6

[a] Vayner et al., ref 8. [b] n.a. denotes not available.

TABLE 2: Aqueous Standard-State Free Energies of Activation (kcal/mol) at 298 K

	R1	**R2**
CBS-QB3/CPCM[a]	40.5	46.9
M06-2X/SM8[b]	36.4	43.5
BMC//M06-2X/SM8[b]	36.5	43.1

[a] Gas-phase geometries. [b] Liquid-phase geometries.

TABLE 3: Components of Aqueous Standard-State Free Energies of Activation (kcal/mol) at 298 K

row	quantity	formula	**R1**	**R2**
1	$\Delta^{\ddagger}G$ (g)		6.5	13.6
2	$\Delta^{\ddagger}G_P$		31.9	28.6
3	$\Delta^{\ddagger}\Delta E_{EN}$		0.3	3.0
4	$\Delta^{\ddagger}\Delta G_{ENP}$	2 + 3	32.2	31.6
5	$\Delta^{\ddagger}G_{CDS}$		−0.3	−0.3
6	$\Delta^{\ddagger}\Delta G_S^*$	4 + 5	31.9	31.3
7	$\Delta^{\ddagger}\Delta G_{conc}$		−1.9	−1.9
8	$\Delta^{\ddagger}\Delta G_S$	6 + 7	30.0	29.4
9	$\Delta^{\ddagger}G$ (aq)	1 + 8	36.5	43.1

was included by the SM8 model. The SM8 calculations require partial atomic charges, and these were obtained by the CM4M charge model.[24] Geometries of reactants and transition states were optimized in both the gas phase and the liquid phase. This first set of calculations will be denoted M06-2X in the gas and SM8/M06-2X in aqueous solution.

In the second set of calculations, the reactant and transition state potential energies at the M06-2X/6-31+G(d,p) gas-phase reactant and saddle point geometries were adjusted by single-point calculations with the BMC-CCSD multicoefficient correlation method.[25] The same correction was also applied in the liquid state. These calculations are denoted BMC//M06-2X for the gas and BMC//SM8/M06-2X for the aqueous solution, where BMC denotes the balanced multicoefficient method.

Software. All calculations were carried out using the Gaussian 03[26] suite of electronic structure programs with local modifications.[27,28]

4. Results

For this and previous work, Table 1 compares, for reactions **R1** and **R2**, the gas-phase potential energy barrier heights, $V^{\ddagger}$ (also called classical barrier heights), the standard-state enthalpies of activation at 0 K, $\Delta^{\ddagger}H_0$ (also called zero-point-inclusive barrier heights), and the standard-state free energies of activation at 298 K, $\Delta^{\ddagger}G_{298}$. Table 2 gives aqueous-phase free energies of activation at 298 K, and Table 3 gives the components of the SM8 calculations of Table 2. Table 4 details the two key geometrical variables of the gas-phase and aqueous transition states, namely, the length of the making and breaking C−Cl bonds (identical by symmetry) and the Cl−C−Cl bond angle. The deviation of the latter variable from 180 , which would be expected for an ideal backside attack, provides some indication of the steric influence of the various substituents. Table 5 provides the chlorine atom partial charges for reactants and transition states.

TABLE 4: Bond Distances and Bond Angles of Partial Bonds at Transition States

	R1		**R2**	
variable	B3LYP	M06-2X	B3LYP	M06-2X
	Gas Phase			
r_{C-Cl}, Å	2.45[a]	2.37	2.54[a]	2.43
$\theta_{Cl-C-Cl}$, deg	161[a]	163	140[a]	148
	Aqueous Phase			
r_{C-Cl}, Å	n.a.[b]	2.40[c]	n.a.[b]	2.49[c]
$\theta_{Cl-C-Cl}$, deg	n.a.[b]	162[c]	n.a.[b]	144[c]

[a] Vayner et al., ref 8. [b] Not given in ref 8. [c] M06-2X/SM8.

TABLE 5: Partial Charges (au)[a] on Cl in M06-2X and M06-2X/SM8 Calculations

phase	**R1**	**R2**
	Reactant	
gas	−1.00, −0.10	−1.00, −0.10
aq//g[b]	−1.00, −0.12	−1.00, −0.11
aqueous	−1.00, −0.12	−1.00, −0.12
	Transition State	
gas	−0.58, −0.58	−0.57, −0.57
aq//g[b]	−0.61, −0.61	−0.62, −0.62
aqueous	−0.61, −0.61	−0.64, −0.64

[a] 1 atomic unit (au) of charge is the charge on a proton. [b] aq//g denotes liquid-phase charges at gas-phase geometries.

5. Analysis and Discussion

5.1. Gas Phase. Our predictions at the M06-2X level and the BMC level are very similar to one another, increasing our confidence in their quantitative utility. The new **R1** results in Table 1 are in excellent agreement with ref 8, and the **R2** free energy of activation is 1.0 kcal/mol higher. Thus, our calculations agree that **R2** should be much slower than **R1** in the gas phase. The BMC calculations predict a slowdown of $\exp(-7.0\ \text{kcal mol}^{-1}/RT)$, which equals 7.3×10^{-6} at 298 K, whereas the measured slowdown in ref 6 is only a factor of 0.16. These results are especially irreconcilable in light of the accuracy shown in validation studies of the various methods used here. In those validation tests,[29] the mean unsigned errors of CBS-QB3, M06-2X/6-31+G(d,p), and BMC-CCSD methods for a diverse representative set of 24 barrier heights are 1.6, 1.5, and 0.7 kcal/mol, respectively, and are even smaller for a subset of six representative barrier heights for S_N2 reactions, in particular, 1.1, 1.4, and 0.5 kcal/mol, respectively.

The gas-phase geometries in Table 4 differ considerably, with B3LYP giving partial bond distances that are 0.08−0.11 Å longer than the present ones. Notably, ref 8 also reports B3LYP geometries for the paradigmatic $Cl^- + CH_3Cl$ transition state, and the listed C−Cl partial bond length, 2.36 Å, is 0.06 Å larger than the most accurate available one for this prototype case, which is 2.30 Å;[30] it is thus reasonable to assume that the B3LYP partial bond distances are similarly too large for **R1** and **R2**. M06-2X/6-31+G(d,p) gives 2.32 Å for the C−Cl bond length at the gas-phase TS for $Cl^- + CH_3Cl$, in much better agreement with the most accurate available values, so we infer similar accuracy here. The longer making and breaking bond length in **R2** compared to **R1** and the greater deviation from 180 for the bond angle θ are consistent with the expected effects of changing the substituent R from CH_3 to $(CH_3)_3C$. In the case of the bond length, the *t*-butyl group provides improved hyperconjugative stabilization of a partial positive charge at the reacting carbon center compared to a methyl group, so the greater ionic character associated with longer C−Cl bonds is

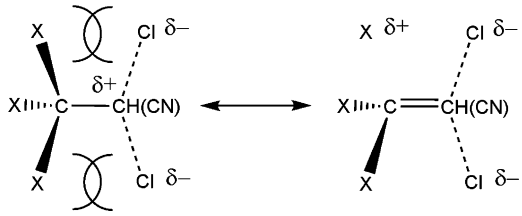

Figure 1. Hyperconjugative resonance in the S_N2 transition-state structure, which will be more stabilizing for X = CH_3 than for X = H, but the larger CH_3 substituent will also introduce unfavorable steric interactions with the Cl atoms as illustrated for the mesomer on the left.

stabilized (Figure 1). In the case of the bond angle, the 15 reduction seen on changing the substituent R from CH_3 to $(CH_3)_3C$ is consistent with the latter group being unable to avoid placing methyl substituents approximately gauche to the making and breaking C−Cl bonds. The observation that B3LYP predicts a bond angle 8 smaller than M06-2X even though it simultaneously predicts longer C−Cl bonds is consistent with the tendency of this functional to overemphasize repulsive aspects of nonbonded interactions by failing to account for dispersion-like medium-range correlation energy.[22,31]

5.2. Aqueous Phase. Table 2 shows agreement to within 4.0 kcal/mol between the present and the previous free energies of activation in the aqueous phase. It is difficult to predict absolute free energies of solvation for ions (in validation tests[16] against 60 anions in aqueous solution, SM8 gave mean unsigned errors of 3.7 kcal/mol with the 6-31G(d) basis set and 3.2 kcal/mol with 6-31+G(d,p), whereas CPCM gave 8.9 kcal/mol with 6-31G(d)), and thus we consider this to be reasonable agreement between the two methods. SM8 predicts aqueous solvation to increase the free energy of activation for each reaction by about 30 kcal/mol.

As shown in Table 4, the making and breaking C−Cl bonds are predicted to be 0.03 and 0.06 Å longer in aqueous solution than in the gas phase for reactions **R1** and **R2**, respectively. An increase in this bond length is consistent with solvation stabilizing separated charge, as the partial charges on the reacting carbon center and the chlorine atoms (see Figure 1) increase with increasing bond distance. The larger effect for **R2** compared to **R1** is consistent with the greater ability of the *t*-butyl group to stabilize partial positive charge on the reacting carbon center. Kormos and Cramer (one of the current authors) observed similar trends in the making and breaking C−Cl bond lengths when studying S_N2 and S_N2' reactions of allylic halides; indeed, they observed that when stabilization of the incipient carbenium ion was sufficiently large, the making and breaking bond lengths became infinite, corresponding to a crossover from S_N2-type reactivity to a preference for S_N1-type ionization.[32] In addition to the bond length changes, the bond angle θ is predicted to decrease by 1−4 in the two TS structures. Such a bond angle decrease is consistent with the tendency for solvation to stabilize aggregation of like charges; however, the change is not very large here, and the potential energy surface is reasonably flat along this coordinate, so we resist overinterpreting this change.

Table 3 shows that the solvation effects on the activation free energies for **R1** and **R2** are entirely dominated by solvent polarization, since $\Delta^{\ddagger}G_{CDS}$ is a very small −0.3 kcal/mol in each case. Moreover, the differential polarization free energies between the TS structures and the reactants $\Delta^{\ddagger}\Delta G_{ENP}$ are very similar for **R1** and **R2**, 32.2 and 31.6 kcal/mol, respectively. In the case of **R1**, the contribution of $\Delta^{\ddagger}\Delta E_{EN}$ to $\Delta^{\ddagger}\Delta G_{ENP}$ is very small, 0.3 kcal/mol, which indicates that the reactants and TS structure are similarly polarizable with respect to gaining solvation free energy from the polarization of the gas-phase structure and electronic density in solution. In the case of **R2**, however, $\Delta^{\ddagger}\Delta E_{EN}$ contributes an order of magnitude larger, 3.0 kcal/mol, to $\Delta^{\ddagger}\Delta G_{ENP}$. This is consistent with the considerably larger change of the solution TS structure relative to the gas phase for **R2** compared to **R1**; geometric relaxation in **R2** changes G_P for the TS structure from −55.1 kcal/mol for the gas phase to −57.7 kcal/mol, while for **R1** the change is from −55.5 to −57.0 kcal/mol. This roughly 50% greater change for **R2**, together with additional effects associated with the reactants, reduces the positive $\Delta^{\ddagger}G_P$ contribution to the activation free energy from 31.9 kcal/mol for **R1** to 28.6 kcal/mol for **R2**, but the additional $\Delta^{\ddagger}\Delta E_{EN}$ cost of the necessary geometric/electronic distortion results in a net $\Delta^{\ddagger}\Delta G_{ENP}$ value for **R2** that is within 0.6 kcal/mol of that for **R1**. Thus, the aqueous solvation effects on the two reaction activation free energies are predicted to be almost identical. We note that at first glance it may appear surprising that the G_P values for the two gas-phase TS structures should be so quantitatively similar to one another, as one might infer from this that the greater dielectric descreening associated with the *t*-butyl group in **R2** compared to the methyl group in **R1** is unimportant. However, it must be recalled that the two TS structures are quite different with respect to the C−Cl making and breaking bond lengths (longer in **R2**) and Cl−C−Cl angle (more acute in **R2**). The geometric changes in **R2** relative to **R1** compensate for the greater dielectric descreening of the *t*-butyl group, and it is coincidental that these different factors lead to a net G_P value close to that for **R1**.

TABLE 6: Substituent Effects on Activation Free Energies (kcal/mol)

level	*t*-Bu−Me
Gas Phase	
CBS-QB3	6.3
BMC//M06-2X	7.1
Aqueous Phase	
CBS-QB3/CPCM	6.4
BMC//M06-2X/SM8	6.6

Table 5 extends this analysis to the effects of geometry and density polarization on the chlorine atom partial charges of the reactants and TS structures. For the reactants in **R1** and **R2**, the partial charge on the chloride ion is obviously invariant at −1, and polarization of the solvated density at the gas-phase geometry leads to an increase in the partial negative charge of the alkyl halide chlorine atom by 0.01−0.02 au. Relaxation of the reactant geometry increases this polarization by less than 0.01 au, which is consistent with the "stiff" nature of the reactant, at least with respect to geometric distortions that might be expected to increase internal charge separation. For the TS structures of **R1** and **R2**, by contrast, larger increases in chlorine atom partial charges are seen: charge polarizations of 0.03 and 0.05 au for **R1** and **R2**, respectively, when the solvated density is relaxed at the gas-phase geometry and an additional 0.02 for **R2** when the TS geometry itself is permitted to relax in solution. Again, as noted above, the larger effects for **R2** are consistent with its looser and more charge-separated character, which is stabilized by the *t*-butyl substituent.

5.3. Substituent Effects. The net substituent effects on activation free energies are summarized in Table 6. For this purpose the substituent effect is defined as $\Delta^{\ddagger}G_{298}$ for **R2** minus $\Delta^{\ddagger}G_{298}$ for **R1**. All substituent effects in the table are in the very narrow range of 6.3−7.1 kcal/mol. Focusing on the most accurate results (BMC//M06-2X), we see that the substituent effect is 7.1 kcal/mol in the gas phase and 6.6 kcal/mol in

TABLE 7: Aqueous Standard-State Free Energies of Activation (kcal/mol) at 298 K

	R3	R4
CBS-QB3/CPCM	38.4	47.6
MC-FEP	23.9	30.4
M06-2X/SM8	34.0	42.0
BMC//M06-2X/SM8	34.3	41.6

solution. Hydrophobic effects and solute−solvent exchange repulsion (i.e., direct steric interaction of solute and solvent) are contained in G_{CDS}; since, as noted above, $\Delta^{\ddagger}G_{CDS}$ is essentially the same for both reactants (accelerating by 0.3 kcal/mol), we conclude that differential hydrophobic effects and direct solute−solvent steric interactions are not important in understanding the contribution of solvation to the substituent effect. Instead, the rather small solvent contribution of −0.5 kcal/mol to the substituent effect can be attributed to electrostatic polarization effects because it is dominated by $\Delta^{\ddagger}\Delta G_{ENP}$, which Table 3 shows to be equal to −0.6 kcal/mol. In terms of absolute solvation free energies for individual species, ΔG_{ENP} is less negative for **R2** than for **R1** by 1.3 kcal/mol for the TS structure (−53.5 vs −54.8 kcal/mol) and by 1.9 kcal/mol for the reactants (−85.1 vs −87.0 kcal, where the difference is entirely associated with the alkyl halide as the chloride ion contributes a constant value in each case), leading to the $\Delta^{\ddagger}\Delta G_{ENP}$ value of −0.6 kcal/mol.

The dielectric descreening effect discussed above is evident in the less negative ΔG_{ENP} values for **R2** compared to those of **R1**. If we were only to examine the partial charges in Table 5, we would expect the opposite ordering in the TS structure because it has larger chlorine partial atomic charges. However, as the *t*-butyl group imposes more dielectric descreening than methyl, the **R2** stationary points either have smaller G_P values or must distort more (and pay the gas-phase cost of that distortion) to offset the descreening effect. We emphasize that dielectric descreening may affect the activation free energy in the same manner as a hydrophobic effect, but physically it is an entirely different phenomenon associated primarily with electrostatics rather than local solvent structure.

6. Another Example

We also considered the S_N2 reactions of Cl^- with $CH_3CH(X)Cl$ and $(CH_3)_3CCH(X)Cl$ for X = H (**R3** and **R4**, respectively) in place of X = CN (**R1** and **R2**, respectively). These reactions are of special interest because they have also been studied in ref 8 by two methods, the CBS-QB3/CPCM method[9] mentioned already and also by Monte Carlo/free energy perturbation theory[33] (MC-FEP). The aqueous free energies of activation are compared in Table 7. The substituent effect, that is, the predicted difference in activation free energy for **R3** versus **R4**, ranges from 6.5 kcal/mol, predicted by MC-FEP, to 9.2 kcal/mol, predicted by CBS-QB3/CPCM. The best SM8 prediction is 7.3 kcal/mol. Again, we focus on physical effects rather than absolute values.

Table 8 provides a breakdown of solvation components for **R3** and **R4** like that in Table 3. The solvation contribution to the substituent effect $\Delta^{\ddagger}\Delta G_S^*$ is +0.6 kcal/mol, which is again dominated by $\Delta^{\ddagger}\Delta G_{ENP}$, which contributes +0.5 kcal/mol. Here, however, the solute geometric/electronic distortion effect $\Delta^{\ddagger}\Delta E_{EN}$ is even greater than for the case of **R1** versus **R2**, contributing +4.2 kcal/mol, which reverses the substituent effect of −3.7 kcal/mol that would be calculated from the raw polarization free energies $\Delta^{\ddagger}G_P$. The interplay between distortion energy and polarization free energy is thus not only quantitatively different in the case of **R3** and **R4** but actually qualitatively different.

TABLE 8: Components of Standard-State Free Energies of Activation (kcal/mol) at 298 K

quantity	R3	R4
$\Delta^{\ddagger}G$ (g)	11.5	18.1
$\Delta^{\ddagger}G_P$	22.1	18.4
$\Delta^{\ddagger}\Delta E_{EN}$	2.8	7.0
$\Delta^{\ddagger}\Delta G_{ENP}$	24.9	25.4
$\Delta^{\ddagger}G_{CDS}$	−0.2	−0.1
$\Delta^{\ddagger}\Delta G_S^*$	24.7	25.3
$\Delta^{\ddagger}\Delta G_{conc}$	−1.9	−1.9
$\Delta^{\ddagger}\Delta G_S$	22.8	23.4
$\Delta^{\ddagger}G$ (aq)	34.3	41.6

The difference between the two sets of reactions must, of course, be attributed to the influence of the CN group compared to H at the reacting center. This difference can be seen in the TS structures. In the gas phase, the making and breaking C−Cl bond lengths are nearly identical for **R1** compared to **R3** and **R2** compared to **R4**; however, the partial charges on the chlorine atoms are not: the gas-phase charges on the Cl atoms in the **R3** and **R4** TS structures are about 0.1 au more negative (each) than in the analogous structures for **R1** and **R2**. There is thus a much greater charge separation in the **R3** and **R4** TS structures, and this separation places positive charge character on the carbenium-like reacting carbon center. The CN group, being inductively electron-withdrawing, suppresses this charge separation in **R1** and **R2**. With larger starting partial charges on the chlorine atoms, there is the potential for greater gains in polarization free energy associated with further loosening the TS structure. Indeed, the SM8 relaxed structures have average making and breaking C−Cl bond lengths of 2.48 Å for **R3** (cf. 2.40 for **R1**) and 2.61 Å for **R4** (cf. 2.49 for **R2**). This causes the raw G_P values to be substantially more negative for the relaxed TS structures of **R3** and **R4** compared to **R1** and **R2**, namely, −61.9 and −64.6 kcal/mol for **R3** and **R4**, respectively (cf. −57.0 and −57.7 kcal/mol for the TS structures of **R1** and **R2**), but the distortion costs are similarly larger.

So, for each set of reactions varying by substitution of a *t*-butyl group for a methyl group, solvation has a fairly small influence on the relative activation free energies because of a cancellation of various effects of modest magnitude on the relevant reactant and TS structures. However, comparing X = H to X = CN, we see that the contribution of aqueous solvation to the activation free energies, $\Delta^{\ddagger}\Delta G_S$, is considerably more positive for **R1** and **R2** (about 30 kcal/mol, see Table 3) than for **R3** and **R4** (about 23 kcal/mol, see Table 8). This trend reflects the reduced charge separation in the TS structures for **R1** and **R2**, caused by CN substitution at the reacting carbon center, which leads to reduced solvation free energies for the TS structures. Interestingly, the net free energies of activation in aqueous solution for **R1** compared to **R3** or for **R2** compared to **R4** are predicted to be within about 2 kcal/mol on one another, because the smaller decelerating influence of water on the X = H reactions roughly compensates for the accelerating gas-phase effect associated with X = CN substitution. This comparison thus represents another example of the typical observation that solvation levels the landscape when energy differences are associated primarily with charge separation.

7. Lessons Learned

The solvent effect on the difference between the S_N2 reaction rates of $CH_3CH(X)Cl$ and $(CH_3)_3CCH(X)Cl$ is small for X =

CN and X = H. The reduced solvation that would be expected from the greater dielectric descreening associated with the larger *t*-butyl group is roughly balanced by the greater tendency of this group to permit geometric and electronic distortion to recapture some of this lost polarization free energy; in magnitude the substituent effect on distortion cancels 82% of the substituent effect on the polarization free energy for X = CN and reverses the sign of the net effect for X = H. A quantitative understanding of these effects requires taking into account all of the changes associated with distortion of the transition-state structures from their gas-phase geometries to their aqueous ones, taking a full account of the volume and shapes of all substituents when calculating the polarization energy. Thus, explanations of substituent effects that use simple models of fixed geometries or spherical, elliptical, or otherwise nondescript cavities would be unlikely to uncover the dominant quantitative aspects.

8. Concluding Remarks

Although the question of steric effects versus solvation effects on S_N2 reactions is more than 70 years old, only recently have all the tools come in place for understanding the problem, and it turns out that computational chemistry provides the required detailed information necessary to dissect the process, although this information is still unavailable experimentally.

To produce reliable results, several advances were required, including (i) the ability to calculate reasonably accurate gas-phase barrier heights for systems with up to eight nonhydrogenic atoms, (ii) the capability to optimize geometries of transition states reliably in both the gas and the liquid solution phases, (iii) the validation of density functionals that correctly estimate medium-range correlation energy so that steric effects and alkyl branching effects are treated properly, (iv) the ability to calculate accurate free energies of solvation, and (v) an appreciation of how to partition solvation effects into quantitatively meaningful contributions from geometric, bulk-electrostatic, and first-solvation-shell effects. An analysis at this level of reliability would not have been possible even a few years ago. It is encouraging that quantum chemistry has now advanced to the point where we can begin to provide nuanced answers to some of the longest-standing questions of mechanistic chemistry.

Acknowledgment. This work was supported in part by the U.S. Department of Energy, Office of Basic Energy Sciences, under Grant No. DE-FG02-86ER13579 (gas-phase studies) and the National Science Foundation under Grants CHE-0610183 and CHE-0704974 (liquid-phase studies).

References and Notes

(1) Hughes, E. D.; Ingold, C. K. *J. Chem. Soc.* **1935**, 244.
(2) Dostrovsky, I.; Hughes, E. D.; Ingold, C. K. *J. Chem. Soc.* **1946**, 173.
(3) Hawkins, G. D.; Cramer, C. J.; Truhlar, D. G. *Chem. Phys. Lett.* **1995**, *246*, 122.
(4) Riveros, J. M.; Jose, J. M.; Takashima, K. *Adv. Phys. Org. Chem.* **1985**, *21*, 197.
(5) Marcus, R. A. *J. Phys. Chem. A* **1997**, *101*, 4072.
(6) Regan, C. K.; Craig, S. L.; Brauman, J. I. *Science* **2002**, *295*, 2245.
(7) Chandresekhar, J.; Smith, S. F.; Jorgensen, W. L. *J. Am. Chem. Soc.* **1985**, *107*, 154.
(8) Vayner, G.; Houk, K. N.; Jorgensen, W. L.; Brauman, J. I. *J. Am. Chem. Soc.* **2004**, *126*, 9054.
(9) Montgomery, J. A.; Frisch, M. J.; Ochtenki, J. W.; Petersson, G. A. *J. Chem. Phys.* **1999**, *110*, 2822.
(10) Barone, V.; Cossi, M. *J. Phys. Chem. A* **1998**, *102*, 1995. Cossi, M.; Adamo, C.; Barone, V. *Chem. Phys. Lett.* **1998**, *297*, 1.
(11) Cramer, C. J.; Truhlar, D. G. *Rev. Comput. Chem.* **1995**, *6*, 1.
(12) Fernandez-Ramos, A.; Ellingson, B. A.; Garrett, B. C.; Truhlar, D. G. *Rev. Comput. Chem.* **2007**, *23*, 125.
(13) Glasstone, S.; Laidler, K.; Eyring, H. *The Theory of Rate Processes*; McGraw-Hill: New York, 1941.
(14) Schenter, G. K.; Garrett, B. C.; Truhlar, D. G. *J. Chem. Phys.* **2003**, *119*, 5828. Chuang, Y.-Y.; Cramer, C. J.; Truhlar, D. G. *Int. J. Quantum Chem.* **1998**, *70*, 887. Cramer, C. J.; Truhlar, D. G. *Chem. Rev.* **1999**, *99*, 2161.
(15) Ben-Naim, A. *Statistical Thermodynamics for Chemists and Biochemists*; Plenum: New York, 1992.
(16) Marenich, A. V.; Olson, R.; Kelly, C. P.; Cramer, C. J.; Truhlar, D. G. *J. Chem. Theory Comput.* **2007**, *3*, 2011.
(17) Cramer, C. J.; Truhlar, D. G. *J. Am. Chem. Soc.* **1991**, *113*, 8305.
(18) Cramer, C. J.; Truhlar, D. G. In *Solvent Effects and Chemical Reactivity*; Tapia, O., Bertrán, J., Eds.; Kluwer: Dordrecht, 1996; p 1.
(19) Marenich, A. V.; Cramer, C. J.; Truhlar, D. G. *J. Chem. Theory Comput.* **2008**, *4*, 877.
(20) Liotard, D. A.; Hawkins, G. D.; Lynch, G. C.; Cramer, C. J.; Truhlar, D. G. *J. Comput. Chem.* **1995**, *16*, 422.
(21) Kohn, W.; Becke, A. D.; Parr, R. G. *J. Phys. Chem.* **1996**, *100*, 12974.
(22) Zhao, Y.; Truhlar, D. G. *Theor. Chem. Acc.* **2008**, *120*, 215. Zhao, Y.; Truhlar, D. G. *Acc. Chem. Res.* **2008**, *41*, 157.
(23) Hehre, W. J.; Radom, L.; Schleyer, P. v. R.; Jople, J. A. *Ab Initio Molecular Orbital Theory*; John Wiley & Sons: Hoboken, 1986.
(24) Olson, R. M.; Marenich, A. V.; Cramer, C. J.; Truhlar, D. G. *J. Chem. Theory Comput.* **2007**, *3*, 2046.
(25) Lynch, B. J.; Zhao, Y.; Truhlar, D. G. *J. Phys. Chem. A* **2005**, *109*, 1643.
(26) Frisch, M. J.; et al. *Gaussian 03*, version E01; Gaussian, Inc.: Wallingford, CT, 2004.
(27) Olson, R. M.; Marenich, A. V.; Chamberlin, A. C.; Kelly, C. P.; Thompson, J. D.; Xidos, J. D.; Li, J.; Hawkins, G. D.; Winget, P. D.; Zhu, T.; Rinaldi, D.; Liotard, D. A.; Cramer, C. J.; Truhlar, D. G.; Frisch, M. J. *MN-GSM*, version 2008; University of Minnesota: Minneapolis, 2008.
(28) Zhao, Y.; Truhlar, D. G. *MN-GFM*, version 3.0; University of Minnesota: Minneapolis, 2006.
(29) Zheng, J.; Zhao, Y.; Truhlar, D. G. *J. Chem. Theory Comput.* **2009**, *5*, 808.
(30) Gonzales, J. M.; Allen, W. D.; Schaefer, H. F. *J. Phys. Chem. A* **2005**, *109*, 10613.
(31) Zhao, Y.; Truhlar, D. G. *Org. Lett.* **2006**, *8*, 5753.
(32) Kormos, B. L.; Cramer, C. J. *J. Org. Chem.* **2003**, *68*, 6375.
(33) Kaminski, G. A.; Jorgensen, W. L. *J. Phys. Chem. B* **1998**, *102*, 1787.

JP905429P